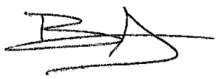
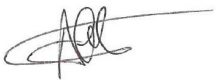
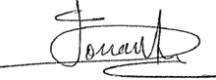


# SEA LEVEL BUDGET CLOSURE - CLIMATE CHANGE INITIATIVE +

## SCIENCE REQUIREMENT DOCUMENT

	Name	Organisation	Date	Visa
Written by :	Antonio Bonaduce, Roshin Raj Benoit Meyssignac Marie Bouih, Anne Barnoud	NERSC LEGOS Magellium	03/07/2024	
Checked by :	Michaël Ablain	Magellium	03/07/2024	
Approved by :	Joël Dorandeu	Magellium	03/07/2024	
Accepted by :	Sarah Connors	ESA		

Document reference:	SLBC_CCI-DT-008-MAG_SRD_D1-1
Edition.Revision:	1.3
Release date:	03/07/2024
Customer:	ESA
Ref. Market, consultation:	ESA AO/1-11340/22/I-NB



## Mailing list

	Name	organisation	Nb. copies
<b>Recipients :</b>	Sarah Connors Marco Restano	ESA	1 (digital)
<b>Internal copy :</b>	Project report	Magellium	1 (digital)

## Document evolution sheet

Ed.	Rev.	Date	Purpose of evolution	Observations
1	0	06/04/2023	Creation of document	
1	1	18/10/2023	ESA review	
1	2	06/06/2024	First year update	Updates on arctic requirements (3.3)
1	3	03/07/2024	ESA review	



## Contents

<b>1. Introduction</b>	<b>6</b>
1.1. Purpose of document	6
1.2. Document structure	6
1.3. Related documents	6
1.3.1. Applicable documents	6
1.3.2. Reference documents	6
1.4. Terminology	10
1.4.1. Acronyms	10
<b>2. Requirements for the sea level budget closure</b>	<b>12</b>
2.1. State-of-the-art of the sea level budget closure	12
2.2. Summary of “How accurate is accurate enough for measuring the sea-level rise and variability” (Meyssignac et al., 2023)	13
2.2.1. Context related to the ESA SLBC_cci+ project	13
2.2.2. Current sea level observing system accuracy and precision	13
2.2.3. Future needs in accuracy and precision	15
2.3. Overview of available data, including new CCI ECVs	17
<b>3. Specific requirements for the Arctic Ocean</b>	<b>19</b>
3.1. State-of-the-art of the Arctic sea level budget closure	19
3.2. Requirements for the altimetry components and ways for improvement	20
3.2.1. The ESA Cryo-TEMPO Project	21
3.2.2. Enhanced altimetry to obtain sea-level signal in sea-ice covered areas	22
3.2.3. The Sea Water and Ocean Topography (SWOT) Mission	23
3.3. Requirements for the gravimetry components and way forward	24
3.4. Requirements for in-situ observations and way forward	26
3.4.1. Tide gauges	26
3.4.2. New phases of the NorArgo Programme	27
3.4.3. Dedicated initiatives to capitalize on the field campaigns collecting data in the Arctic	29
3.4.3.1. Beaufort Gyre Exploration Project	29
3.4.3.2. GoNorth expeditions	29
3.4.3.3. HiAOOS Project	30
<b>4. Summary</b>	<b>30</b>

## List of tables

Table 1: List of applicable documents	6
Table 2: List of acronyms.	11
Table 3: Science questions and their needs in terms of sea level estimates' accuracy, from Meyssignac et al. (2023).	16
Table 4: Available datasets for the sea level budget components. Improvements foreseen in the SLBC_cci+ projects are indicated in bold font. Available CCI ECVs are written in blue.	18

## List of figures

Figure 1: Uncertainty in global mean sea level trends computed over any period > 5 years included in 1993-2020 (adapted from Guérou et al. 2022, the central year of the period used to compute the trend is in the x-axis and the length of the period is in the y-axis), extracted from Meyssignac et al. (2023).	14
Figure 2: Uncertainty at the 66% CL in sea level trends computed over different length periods that are all ending in 2020 and partitioning of the uncertainty among different sources: 2-months and 1-year correlated noises ("CN 2-m/1-yr", coming essentially from the radar altimeter errors), the radiometer WTC, the intermission offsets, the GIA, the ITRF, extracted from Meyssignac et al. (2023).	15
Figure 3: Arctic Sea level Budget: Area averaged monthly sea level (red), the sum of GSFC ocean mass change and the EN4 steric height estimates (SHOM, blue), and the residual (green) for the entire Arctic during the time period 2003–2016. The dashed vertical line indicates the separation of the time periods 2003-2009 and 2010-2016 when changes in the dominant atmospheric patterns over the Arctic are observed (from Raj et al., 2020).	20
Figure 4: The panels show the Sea level anomaly (SLA) trend (mm/yr) for the time period 2003–2016 with the marked locations of the Beaufort Gyre (BG), the Nordic Seas (NS), Barents Sea (BS) and the Russian shelf region (RS). SLA trends (mm/yr) of percentile 2.5% (b) and 97.5% (c) for the same time period. the sea level anomaly trend for the time period 2003–2016 with the marked locations of the Beaufort Gyre (BG), the Nordic Seas (NS), Barents Sea (BS) and the Russian shelf region (RS); The trend estimates are obtained from conventional altimetry maps; values expressed as mm yr-1 (from Raj et al., 2020).	21
Figure 5: Sea-level anomaly (cm) in the Arctic. The values show the sea-level anomalies, averaged over a period spanned by the Cryosat and Cryosat-2 missions (2010-2021).The map is obtained by binning (every 1-degree longitude and 0.5-degree latitude bins) along-track data of the altimetry missions which have been reprocessed, in the framework of the ESA Cryo-Tempo project to account for the	22

sea-level signal in the sea-ice covered areas and reduce the polar gap. The black frames represent the Beaufort Sea (BS) and the Eurasian Basin (EB) domains.

Figure 6: Mean Arctic SLA maps for SRL (a), S3A (b) and C2 (c). All maps are estimated over the time span common to all missions (July 2016–April 2019) (Prandi et al., 2021). 22

Figure 7: The black outlined area including the Lofoten Basin shows the geographical domain where satellite sensor synergy data are collocated with Argo profiling floats. Arrows mark the flow directions of the Norwegian Coastal Current (green), Norwegian-Atlantic Current (red) East Greenland Current (blue) and Deep overflow water (black). 23

Figure 8: The panels show the SWOT KaRIN image in the Lofoten Basin during four consecutive days in May 2023 (8th-11th May 2023, clockwise from top-left). The patterns show the variability of the absolute dynamic topography (ADT) in the area. While the processing of SWOT KaRIN images is still preliminary, early images can be accessed through a dedicated bulletin for a number of early adopter initiatives: ([https://bulletin.aviso.altimetry.fr/html/produits/swot/adac/welcome\\_uk.php](https://bulletin.aviso.altimetry.fr/html/produits/swot/adac/welcome_uk.php)). 24

Figure 9: GSFC (left panels) and ITSG (right panels) derived ocean mass trend during the two time-periods 2003-2009 (upper panels) and 2010-2016 (lower panels). 25

Figure 10: Top panel: Map showing the location of the PSMSL tide gauges in the Arctic region (defined as the region to the north of 66°N). Bottom panel: A bar chart with the number of tide-gauge observations in the Arctic region for each month between January 1993 and December 2022 (PSMSL tide gauges do not contain values after Dec 2021). Two out of the one hundred PSMSL tide gauges do not contain values over the period considered. These two tide gauges are located near the border between Norway and Russia. Their location is shown on the map with empty red circles. 27

Figure 11: Registered positions of all operative Argo floats in the world ocean (April 2023). 28

Figure 12: The panel shows an example profiling floats of the NorArgo operating in the Nordic Seas during a day ([www.imr.no/forskning/prosjekter/norargo/map](http://www.imr.no/forskning/prosjekter/norargo/map)). 29

# 1. Introduction

## 1.1. Purpose of document

This document is the Science Requirements Document (SRD) for the ESA SLBC\_cci+ project ([AD-1] and [AD-2]). It aims at presenting the state-of-the-art of the sea level budget closure (SLBC) and at establishing the foreseen science requirements for the SLBC\_cci+ in terms of data and uncertainties.

## 1.2. Document structure

In addition to this introduction, this document includes the following sections:

- Section 2 describes the requirements for the SLBC starting by a state-of-the-art. A description of the requirements is given, focusing on the altimetric component, followed by a discussion of data availability and the use of the essential climate variables (ECVs) recently provided by the ESA Climate Change Initiative (CCI) program.
- Section 3 presents the specific requirements for the sea level budget in the Arctic Ocean. This section starts by a state-of-the-art of the SLBC in the Arctic Ocean and then describes requirements for altimetric, gravimetric and in-situ observations.

## 1.3. Related documents

### 1.3.1. Applicable documents

Id.	Ref.	Description
[AD-1]	ESA AO/1-11340/22/I-NB	Call to tender "SEA LEVEL BUDGET CLOSURE_CCI+ (SLBC_CCI+)"
[AD-2]	MAG-22-PTF-060_DetailedProposal_V2	Detailed proposal in response to ESA/ESRIN Request for Quotation "SEA LEVEL BUDGET CLOSURE_CCI+ (SLBC_CCI+)" ESA AO/1-11340/22/I-NB [AD-1]

Table 1: List of applicable documents

### 1.3.2. Reference documents

Ablain, M., Meyssignac, B., Zawadzki, L., Jugier, R., Ribes, A., Spada, G., Benveniste, J., Cazenave, A., and Picot, N.: Uncertainty in satellite estimates of global mean sea-level changes, trend and acceleration, *Earth Syst. Sci. Data*, 11, 1189–1202, <https://doi.org/10.5194/essd-11-1189-2019>, 2019.

Bamber, J. L., Westaway, R. M., Marzeion, B., and Wouters, B.: The land ice contribution to sea

- level during the satellite era, *Environ. Res. Lett.*, 13, 063008, <https://doi.org/10.1088/1748-9326/aac2f0>, 2018.
- Barnoud, A., Pfeffer, J., Guérou, A., Frery, M.-L., Siméon, M., Cazenave, A., Chen, J., Llovel, W., Thierry, V., Legeais, J.-F., and Ablain, M.: Contributions of altimetry and Argo to non-closure of the global mean sea level budget since 2016, *Geophys. Res. Lett.*, <https://doi.org/10.1029/2021gl092824>, 2021.
- Barnoud, A., Pfeffer, J., Cazenave, A., Fraudeau, R., Rousseau, V., and Ablain, M.: Revisiting the global mean ocean mass budget over 2005–2020, *Ocean Sci.*, 19, 321–334, <https://doi.org/10.5194/os-19-321-2023>, 2023.
- Bonaduce, A., Benkiran, M., Remy, E., Le Traon, P. Y., and Garric, G.: Contribution of future wide-swath altimetry missions to ocean analysis and forecasting, *Ocean Sci.*, 14, 1405–1421, <https://doi.org/10.5194/os-14-1405-2018>, 2018.
- Camargo, C. M. L., Riva, R. E. M., Hermans, T. H. J., Schütt, E. M., Marcos, M., Hernandez-Carrasco, I., and Slangen, A. B. A.: Regionalizing the sea-level budget with machine learning techniques, *Ocean Sci.*, 19, 17–41, <https://doi.org/10.5194/os-19-17-2023>, 2023.
- Cazenave, A., Dieng, H.-B., Meyssignac, B., von Schuckmann, K., Decharme, B., and Berthier, E.: The rate of sea-level rise, *Nat. Clim. Change*, 4, 358–361, <https://doi.org/10.1038/nclimate2159>, 2014.
- Chambers, D. P., Cazenave, A., Champollion, N., Dieng, H., Llovel, W., Forsberg, R., von Schuckmann, K., and Wada, Y.: Evaluation of the Global Mean Sea Level Budget between 1993 and 2014, *Surv. Geophys.*, 38, 309–327, <https://doi.org/10.1007/s10712-016-9381-3>, 2017.
- Chen, J., Tapley, B., Wilson, C., Cazenave, A., Seo, K.-W., and Kim, J.-S.: Global Ocean Mass Change From GRACE and GRACE Follow-On and Altimeter and Argo Measurements, *Geophys. Res. Lett.*, 47, e2020GL090656, <https://doi.org/10.1029/2020GL090656>, 2020.
- Cornish, S. B., Muilwijk, M., Scott, J. R., Marson, J. M., Myers, P. G., Zhang, W., Wang, Q., Kostov, Y., Johnson, H. L., and Marshall, J.: Impact of sea ice transport on Beaufort Gyre liquid freshwater content, *Clim. Dyn.*, 61, 1139–1155, <https://doi.org/10.1007/s00382-022-06615-4>, 2023.
- Dieng, H. B., Cazenave, A., Meyssignac, B., and Ablain, M.: New estimate of the current rate of sea level rise from a sea level budget approach, *Geophys. Res. Lett.*, 44, 3744–3751, <https://doi.org/10.1002/2017gl073308>, 2017.
- Donlon, C., Berruti, B., Buongiorno, A., Ferreira, M.-H., Féménias, P., Frerick, J., Goryl, P., Klein, U., Laur, H., Mavrocordatos, C., Nieke, J., Rebhan, H., Seitz, B., Stroede, J., and Sciarra, R.: The Global Monitoring for Environment and Security (GMES) Sentinel-3 mission, *Remote Sens. Environ.*, 120, 37–57, <https://doi.org/10.1016/j.rse.2011.07.024>, 2012.
- Donlon, C. J., Cullen, R., Giulicchi, L., Vuilleumier, P., Francis, C. R., Kuschnerus, M., Simpson, W., Bouridah, A., Caleno, M., Bertoni, R., Rancaño, J., Pourier, E., Hyslop, A., Mulcahy, J., Knockaert, R., Hunter, C., Webb, A., Fornari, M., Vaze, P., Brown, S., Willis, J., Desai, S., Desjonqueres, J.-D., Scharroo, R., Martin-Puig, C., Leuliette, E., Egido, A., Smith, W. H. F., Bonnefond, P., Le Gac, S., Picot, N., and Tavernier, G.: The Copernicus Sentinel-6 mission: Enhanced continuity of satellite sea level measurements from space, *Remote Sens. Environ.*, 258, 112395, <https://doi.org/10.1016/j.rse.2021.112395>, 2021.
- Douglas, B. C.: Global sea level rise, *J. Geophys. Res. Oceans*, 96, 6981–6992, <https://doi.org/10.1029/91JC00064>, 1991.
- Douglas, B. C.: GLOBAL SEA RISE: A REDETERMINATION, *Surv. Geophys.*, 18, 279–292, <https://doi.org/10.1023/A:1006544227856>, 1997.
- Dussaillant, I., Bannwart, J., Paul, F., and Zemp, M.: Glacier mass change global gridded data from 1976 to present derived from the Fluctuations of Glaciers Database. World Glacier Monitoring Service., 2023.
- Fasullo, J. T. and Nerem, R. S.: Altimeter-era emergence of the patterns of forced sea-level rise in climate models and implications for the future, *Proc. Natl. Acad. Sci.*, 115, 12944–12949, <https://doi.org/10.1073/pnas.1813233115>, 2018.
- Forget, G. and Ponte, R. M.: The partition of regional sea level variability, *Prog. Oceanogr.*, 137,

- 173–195, <https://doi.org/10.1016/j.pocean.2015.06.002>, 2015.
- Forster, P., Storelvmo, T., Armour, K., Collins, W., Dufresne, J.-L., Frame, D., Lunt, D., Mauritsen, T., Palmer, M., and Watanabe, M.: The Earth's energy budget, climate feedbacks, and climate sensitivity, 2021.
- Fox-Kemper, B., Hewitt, H. T., Xiao, C., Adalgeirsdottir, G., Drijfhout, S. S., Edwards, T. L., Golledge, N. R., Hemer, M., Kopp, R. E., Krinner, G., Mix, A., Notz, D., Nowicki, S., Nurhati, I. S., Ruiz, L., Sallée, J.-B., Slangen, A. B. A., and Yu, Y.: Ocean, Cryosphere and Sea Level Change., in: *Climate Change 2021: The Physical Science Basis. Contribution of Working Group I to the Sixth Assessment Report of the Intergovernmental Panel on Climate Change*, edited by: Masson-Delmotte, V., Zhai, P., Pirani, A., Connors, S. L., Péan, C., Berger, S., Caud, N., Chen, Y., Goldfarb, L., Gomis, M. I., Huang, M., Leitzell, K., Lonnoy, E., Matthews, J. B. R., Maycock, T. K., Waterfield, T., Yelekci, O., Yu, R., and Zhou, B., Cambridge University Press, Cambridge, United Kingdom and New York, NY, USA, 1211–1362, <https://doi.org/10.1017/9781009157896.011>, 2021.
- Frederikse, T., Landerer, F., Caron, L., Adhikari, S., Parkes, D., Humphrey, V. W., Dangendorf, S., Hogarth, P., Zanna, L., Cheng, L., and Wu, Y.-H.: The causes of sea-level rise since 1900, *Nature*, 584, 393–397, <https://doi.org/10.1038/s41586-020-2591-3>, 2020.
- Groh, A. and Horwath, M.: The method of tailored sensitivity kernels for GRACE mass change estimates, EPSC2016-12065, 2016.
- Guérou, A., Meyssignac, B., Prandi, P., Ablain, M., Ribes, A., and Bignalet-Cazalet, F.: Current observed global mean sea level rise and acceleration estimated from satellite altimetry and the associated uncertainty, *All Depths/Remote Sensing/All Geographic Regions/Sea level/Oceans and climate*, <https://doi.org/10.5194/egusphere-2022-330>, 2022.
- Hakuba, M. Z., Frederikse, T., and Landerer, F. W.: Earth's Energy Imbalance From the Ocean Perspective (2005–2019), *Geophys. Res. Lett.*, 48, e2021GL093624, <https://doi.org/10.1029/2021GL093624>, 2021.
- Hamlington, B. D., Frederikse, T., Nerem, R. S., Fasullo, J. T., and Adhikari, S.: Investigating the Acceleration of Regional Sea Level Rise During the Satellite Altimeter Era, *Geophys. Res. Lett.*, 47, <https://doi.org/10.1029/2019GL086528>, 2020.
- Hart-Davis, M., Howard, S. L., Ray, R., Andersen, O., Padman, L., Nilsen, F., and Dettmering, D.: Arctic Tidal Constituent Atlas (ArcTiCA): A database of tide elevation constituents for the Arctic region from 1800 through present day., <https://doi.org/10.18739/A2D795C4N>, 2023.
- Holgate, S. J., Matthews, A., Woodworth, P. L., Rickards, L. J., Tamisiea, M. E., Bradshaw, E., Foden, P. R., Gordon, K. M., Jevrejeva, S., and Pugh, J.: New Data Systems and Products at the Permanent Service for Mean Sea Level, *J. Coast. Res.*, 29, 493–504, <https://doi.org/10.2112/JCOASTRES-D-12-00175.1>, 2013.
- Horwath, M., Gutknecht, B. D., Cazenave, A., Palanisamy, H. K., Marti, F., Marzeion, B., Paul, F., Bris, R. L., Hogg, A. E., Otosaka, I., Shepherd, A., Döll, P., Cáceres, D., Schmied, H. M., Johannessen, J. A., Nilsen, J. E. Ø., Raj, R. P., Forsberg, R., Sørensen, L. S., Barletta, V. R., Simonsen, S. B., Knudsen, P., Andersen, O. B., Randall, H., Rose, S. K., Merchant, C. J., Macintosh, C. R., Schuckmann, K. von, Novotny, K., Groh, A., Restano, M., and Benveniste, J.: Global sea-level budget and ocean-mass budget, with focus on advanced data products and uncertainty characterisation, *Earth Syst. Sci. Data*, 14, 411–447, <https://doi.org/10.5194/essd-14-411-2022>, 2022.
- Hugonnet, R., McNabb, R., Berthier, E., Menounos, B., Nuth, C., Girod, L., Farinotti, D., Huss, M., Dussallant, I., Brun, F., and Käab, A.: Accelerated global glacier mass loss in the early twenty-first century, *Nature*, 592, 726–731, <https://doi.org/10.1038/s41586-021-03436-z>, 2021.
- Humphrey, V. and Gudmundsson, L.: GRACE-REC: a reconstruction of climate-driven water storage changes over the last century, *Earth Syst. Sci. Data*, 11, 1153–1170, <https://doi.org/10.5194/essd-11-1153-2019>, 2019.
- Johnson, G. C. and Chambers, D. P.: Ocean bottom pressure seasonal cycles and decadal trends from GRACE Release-05: Ocean circulation implications, *J. Geophys. Res. Oceans*, 118, 4228–4240, <https://doi.org/10.1002/jgrc.20307>, 2013.



- Kvas, A., Behzadpour, S., Ellmer, M., Klinger, B., Strasser, S., Zehentner, N., and Mayer-Gürr, T.: ITSG-Grace2018: Overview and Evaluation of a New GRACE-Only Gravity Field Time Series, *J. Geophys. Res. Solid Earth*, 124, 9332–9344, <https://doi.org/10.1029/2019JB017415>, 2019.
- Leuliette, E. W., Nerem, R. S., and Mitchum, G. T.: Calibration of TOPEX/Poseidon and Jason Altimeter Data to Construct a Continuous Record of Mean Sea Level Change, *Mar. Geod.*, 27, 79–94, <https://doi.org/10.1080/01490410490465193>, 2004.
- Loeb, N. G., Thorsen, T. J., Norris, J. R., Wang, H., and Su, W.: Changes in Earth's Energy Budget during and after the “Pause” in Global Warming: An Observational Perspective, *Climate*, 6, 62, <https://doi.org/10.3390/cli6030062>, 2018a.
- Loeb, N. G., Doelling, D. R., Wang, H., Su, W., Nguyen, C., Corbett, J. G., Liang, L., Mitrescu, C., Rose, F. G., and Kato, S.: Clouds and the Earth's Radiant Energy System (CERES) Energy Balanced and Filled (EBAF) Top-of-Atmosphere (TOA) Edition-4.0 Data Product, *J. Clim.*, 31, 895–918, <https://doi.org/10.1175/JCLI-D-17-0208.1>, 2018b.
- Loeb, N. G., Johnson, G. C., Thorsen, T. J., Lyman, J. M., Rose, F. G., and Kato, S.: Satellite and Ocean Data Reveal Marked Increase in Earth's Heating Rate, *Geophys. Res. Lett.*, 48, e2021GL093047, <https://doi.org/10.1029/2021GL093047>, 2021.
- Loomis, B. D., Luthcke, S. B., and Sabaka, T. J.: Regularization and error characterization of GRACE mascons, *J. Geod.*, 93, 1381–1398, <https://doi.org/10.1007/s00190-019-01252-y>, 2019.
- Luthcke, S. B., Sabaka, T. J., Loomis, B. D., Arendt, A. A., McCarthy, J. J., and Camp, J.: Antarctica, Greenland and Gulf of Alaska land-ice evolution from an iterated GRACE global mascon solution, *J. Glaciol.*, 59, 613–631, <https://doi.org/10.3189/2013JoG12J147>, 2013.
- Mangini, F., Bonaduce, A., Chafik, L., Raj, R., and Bertino, L.: Detection and attribution of intra-annual mass component of sea-level variations along the Norwegian coast, *Sci. Rep.*, 13, 15334, <https://doi.org/10.1038/s41598-023-40853-8>, 2023.
- Marti, F., Blazquez, A., Meyssignac, B., Ablain, M., Barnoud, A., Fraudeau, R., Jugier, R., Chenal, J., Larnicol, G., Pfeffer, J., Restano, M., and Benveniste, J.: Monitoring the ocean heat content change and the Earth energy imbalance from space altimetry and space gravimetry, *Earth Syst. Sci. Data*, 14, 229–249, <https://doi.org/10.5194/essd-14-229-2022>, 2022.
- Meyssignac, B., Boyer, T., Zhao, Z., Hakuba, M. Z., Landerer, F. W., Stammer, D., Köhl, A., Kato, S., L'Ecuyer, T., Ablain, M., Abraham, J. P., Blazquez, A., Cazenave, A., Church, J. A., Cowley, R., Cheng, L., Domingues, C. M., Giglio, D., Gouretski, V., Ishii, M., Johnson, G. C., Killick, R. E., Legler, D., Llovel, W., Lyman, J., Palmer, M. D., Piotrowicz, S., Purkey, S. G., Roemmich, D., Roca, R., Savita, A., Schuckmann, K. von, Speich, S., Stephens, G., Wang, G., Wijffels, S. E., and Zilberman, N.: Measuring Global Ocean Heat Content to Estimate the Earth Energy Imbalance, *Front. Mar. Sci.*, 6, <https://doi.org/10.3389/fmars.2019.00432>, 2019.
- Mitchum, G. T.: Comparison of TOPEX sea surface heights and tide gauge sea levels, *J. Geophys. Res. Oceans*, 99, 24541–24553, <https://doi.org/10.1029/94JC01640>, 1994.
- Mitchum, G. T.: Monitoring the Stability of Satellite Altimeters with Tide Gauges, *J. Atmospheric Ocean. Technol.*, 15, 721–730, [https://doi.org/10.1175/1520-0426\(1998\)015<0721:MTSOSA>2.0.CO;2](https://doi.org/10.1175/1520-0426(1998)015<0721:MTSOSA>2.0.CO;2), 1998.
- Mitchum, G. T.: An Improved Calibration of Satellite Altimetric Heights Using Tide Gauge Sea Levels with Adjustment for Land Motion, *Mar. Geod.*, 23, 145–166, <https://doi.org/10.1080/01490410050128591>, 2000.
- Palca, J.: Ocean satellites: Topex launch comes closer, *Nature*, 322, 9–9, <https://doi.org/10.1038/322009b0>, 1986.
- Prandi, P., Meyssignac, B., Ablain, M., Spada, G., Ribes, A., and Benveniste, J.: Local sea level trends, accelerations and uncertainties over 1993–2019, *Sci. Data*, 8, 1, <https://doi.org/10.1038/s41597-020-00786-7>, 2021.
- Raj, R., Andersen, O., Johannessen, J., Gutknecht, B., Chatterjee, S., Rose, S., Bonaduce, A., Horwath, M., Ranndal, H., Richter, K., Palanisamy, H., Ludwigsen, C., Bertino, L., Ø. Nilsen, J., Knudsen, P., Hogg, A., Cazenave, A., and Benveniste, J.: Arctic Sea Level Budget Assessment during the GRACE/Argo Time Period, *Remote Sens.*, 12, 2837,

<https://doi.org/10.3390/rs12172837>, 2020.

Raj, R. P., Johannessen, J. A., Eldevik, T., Nilsen, J. E. Ø., and Halo, I.: Quantifying mesoscale eddies in the Lofoten Basin, *J. Geophys. Res. Oceans*, 121, 4503–4521, <https://doi.org/10.1002/2016JC011637>, 2016.

Roemmich, D., Johnson, G. C., Riser, S., Davis, R., Gilson, J., OWENS, W. B., GARZOLI, S. L., SCHMID, C., and IGNASZEWSKI, M.: The Argo Program, *Oceanography*, 22, 34–43, 2009.

Royston, S., Vishwakarma, B. D., Westaway, R., Rougier, J., Sha, Z., and Bamber, J.: Can We Resolve the Basin-Scale Sea Level Trend Budget From GRACE Ocean Mass?, *J. Geophys. Res. Oceans*, 125, <https://doi.org/10.1029/2019jc015535>, 2020.

Slangen, A. B. A., Church, J. A., Agosta, C., Fettweis, X., Marzeion, B., and Richter, K.: Anthropogenic forcing dominates global mean sea-level rise since 1970, *Nat. Clim. Change*, 6, 701–705, <https://doi.org/10.1038/nclimate2991>, 2016.

Tapley, B. D., Bettadpur, S., Watkins, M., and Reigber, C.: The gravity recovery and climate experiment: Mission overview and early results, *Geophys. Res. Lett.*, 31, n/a-n/a, <https://doi.org/10.1029/2004gl019920>, 2004.

WCRP Global Sea Level Budget Group: Global sea-level budget 1993–present, *Earth Syst. Sci. Data*, 10, 1551–1590, <https://doi.org/10.5194/essd-10-1551-2018>, 2018.

Wunsch, C.: Global Ocean Integrals and Means, with Trend Implications, *Annu. Rev. Mar. Sci.*, 8, 1–33, <https://doi.org/10.1146/annurev-marine-122414-034040>, 2016.

## 1.4. Terminology

### 1.4.1. Acronyms

The list of acronyms that are used in the document is presented in the following table (Table 2).

Acronym	Description
C3S	Copernicus Climate Change Service
CCI	The ESA Climate Change Initiative
CDR	Climate Data Records
CERES	Clouds and the Earth's Radiant Energy System
CL	Confidence Level
ECV	Essential Climate Variable
EEI	Earth energy imbalance
ESA	European Space Agency
GHG	Greenhouse gas
GIA	Glacial Isostatic Adjustment
GMSL	Global Mean Sea Level
GRACE	Gravity Recovery and Climate Experiment

GRACE-FO	GRACE Follow-On
HiAOOS	High Arctic Ocean Observation System
ITRF	International Terrestrial Reference Frame
SAR	Synthetic Aperture Radar
SLA	Sea Level Anomaly
SLB	Sea level budget
SLBC	Sea level budget closure
SLBC_cci	Sea Level Budget Closure of the ESA Climate Change Initiative (first phase)
SLBC_cci+	Sea Level Budget Closure of the ESA Climate Change Initiative (second phase, this activity)
SL_cci	The Sea Level component of the ESA Climate Change Initiative
SRD	Science Requirement Document
WCRP	World Climate Research Programme
WP	Work Package
WTC	Wet Troposphere Correction

Table 2: List of acronyms.

## 2. Requirements for the sea level budget closure

### 2.1. State-of-the-art of the sea level budget closure

The oceans on Earth absorb around 91% of the excess of energy due to the top of the atmosphere radiation imbalance, while only about 3% of the excess of energy ends up melting ice (IPCC, Forster et al., 2021). Over 2006-2018, the former which causes the ocean thermal expansion was responsible for one third of the global mean sea level (GMSL) rise and the latter was responsible for two thirds of the GMSL rise (Fox-Kemper et al., 2021). Therefore, sea level is a crucial indicator of climate change, integrating effects of changes in several climate system components. Assessing the consistency of the observing system and attributing sea level change to its different drivers is typically accomplished using a sea level budget approach (Chambers et al., 2017; WCRP Global Sea Level Budget Group, 2018).

The sea level budget approach consists in comparing the total sea level variations observed by altimetry data with the sum of the steric sea level change due to temperature and salinity variations observed by in situ oceanographic measurements and of the manometric sea level change due to ocean mass variations observed by GRACE and GRACE Follow-On (GRACE-FO) satellite gravimetry missions since 2002. In situ temperature and salinity measurements have been performed by different networks and campaigns, including the Argo network which has been fully deployed since 2005. Before the launch of GRACE gravimetry mission, the barystatic sea level, i.e. the global mean manometric sea level, can be estimated by summing the individual mass contributions to sea level change, namely Greenland and Antarctica ice mass changes, other land glaciers ice mass changes, land water storage variations and atmosphere water vapour content changes. The global mean sea level budget over the period 1993-2020 has been analyzed for several years. Until 2015/2016, the GMSL budget was closed within the uncertainties of the sea level budget components (e.g. Horwath et al., 2022). However, beyond 2016 the budget comparing altimetry, Argo, GRACE and GRACE-FO observations does not close anymore (e.g. Chen et al., 2020). Part of the non-closure has been attributed to drifts in Argo salinity measurements (Barnoud et al., 2021) and in Jason-3 altimetry mission wet troposphere correction (Barnoud et al., 2023). The remaining non-closure of the GMSL budget observed in recent years could also result from errors in altimetry, gravimetry and Argo data.

While the GMSL budget for the period 1993-2016 is considered closed, there are still significant differences between the total measured change and the sum of its contributions at local scale (Frederikse et al., 2020). This disparity is partially due to the limited spatio-temporal resolution of current observational systems in capturing the components and processes involved in the sea level budget, which limits the closure on a local spatial scale, such as  $1^{\circ} \times 1^{\circ}$  resolution (Royston et al., 2020). Previous analyses of the regional sea level budget have mainly been analyzed on basin-wide scales (e.g. Royston et al., 2020; Frederikse et al., 2020), showing closure of the budget in most ocean basins, except in the Indian, South Pacific and Arctic Oceans. A recent study by Camargo et al. (2023) has examined the sea level budget on sub-basin scales worldwide, using a reconstruction of ocean mass instead of GRACE data. By identifying smaller regions with

coherent sea level variability, they were able to eliminate some of the effects of small-scale variability, enabling a closure of the budget at a sub-basin scale.

The ESA SLBC\_cci+ project aims at extending the global mean sea level budget with up-to-date data and at assessing the sea level budget at regional scale. A particular attention will be paid to the estimate of the uncertainties of each component and of the uncertainties due to the observability of the system.

## 2.2. Summary of “How accurate is accurate enough for measuring the sea-level rise and variability” (Meyssignac et al., 2023)

### 2.2.1. Context related to the ESA SLBC\_cci+ project

Meyssignac et al. (2023) detailed the requirements to address three scientific questions, related to the sea level budget closure: the closure of the sea level budget itself, the detection and attribution of sea level rise to greenhouse gas (GHG) emissions and the monitoring of the Earth’s energy imbalance. This review is summarized in the present section. Note that the study of Meyssignac et al. (2023) focuses on the altimetry component of the sea level budget, in the sense that the uncertainty requirements are fully attributed to the altimetry component only, neglecting the uncertainties of the other components of the sea level budget. Within the scope of the SLBC\_cci+, the uncertainty requirements presented in Table 3 (section 2.2.2) are to be applied to the budget residuals, integrating the uncertainties of all components involved in the computation of the sea level budget not only the altimetry component.

### 2.2.2. Current sea level observing system accuracy and precision

The launch of the TopEx/Poseidon mission in August 1992 opened a new era in oceanography and sea level science (Palca, 1986). It used on-board microwave radiometers to measure the atmospheric water content along the same path as the radar signal, as well as precise orbit tracking by different instruments. This enabled for the first time to remotely measure absolute sea level changes in the ITRF with an accuracy of a few centimeters, on a global basis, every 10 days. At larger spatial scales, it revealed oceanic signals of amplitude smaller than a few cm, such as the asymmetric seasonal cycle in sea level, the interannual variability of sea level in response to major climate modes of variability, the reduction of sea level in response to major volcanic eruptions and a persistent increase in the global mean sea level of 3 to 4 mm/yr (Cazenave et al., 2014). By monitoring such small signals, satellite altimetry enabled for the first time to quantify the response of sea level to the changes in the global earth energy cycle and water cycle (Horwath et al., 2022)

During the 2000s, the Argo network (Roemmich et al., 2009) and the launch of the GRACE mission (Tapley et al., 2004) provided two significant improvements in the ocean observing system. Since 2005, the availability of both Argo data and GRACE data allowed to partition sea level changes into thermal expansion and ocean mass changes and to verify, by comparing with satellite altimetry

data, that the sum of these contributions explain total sea level changes within uncertainties (Cazenave et al., 2014).

Closing the SLB at annual and longer time scales, at a useful level of accuracy, became an essential and central problem of modern physical oceanography for three reasons: to guarantee that all important causes for sea level variability are identified and that their combination matches total sea level changes; to cross-validate worldwide complex observing systems such as the Argo network, the space gravimetry missions GRACE/GRACE-FO and the satellite altimetry system; and to test the consistency of different observed variables of the climate system including sea level, ocean temperature and ocean mass, with regard to conservation laws including those of mass, energy and freshwater.

16 satellite altimeters have flown since TopEx/Poseidon, including the Jason satellite series, the Sentinel 3A/B satellites of the European Copernicus programme (Donlon et al., 2021), and the recently launched Sentinel 6-Michael Freilich mission (Donlon et al., 2012). New synthetic aperture radar (SAR) techniques employed by Sentinel-3 and Sentinel-6 altimeters provide access to measurements with improved uncertainty and with higher along track sampling compared to previous low resolution mode systems. For a single 1Hz measurement, the precision is between 2 cm and 2.5 cm at the 90% confidence level (CL) and the accuracy is between 2.5 cm and 3.5 cm at the 90% CL (Ablain et al., 2019). On time scales longer than 1s and spatial scales larger than the footprint of the radar echo, measurement errors show an important correlation across time and space that is essential to evaluate in order to derive the uncertainty in sea level estimates at time scales longer than one year. Now the error variance-covariance matrix of satellite altimetry is available from 1993 to 2021, for the GMSL (Guérou et al., 2022) and for yearly 2°x2° sea level grids (Prandi et al., 2021). On monthly time scale, GMSL uncertainty estimates show a decrease from 9 mm (90% CL) in 1993 to 3 mm (90% CL) in 2015 (see Figure 1).

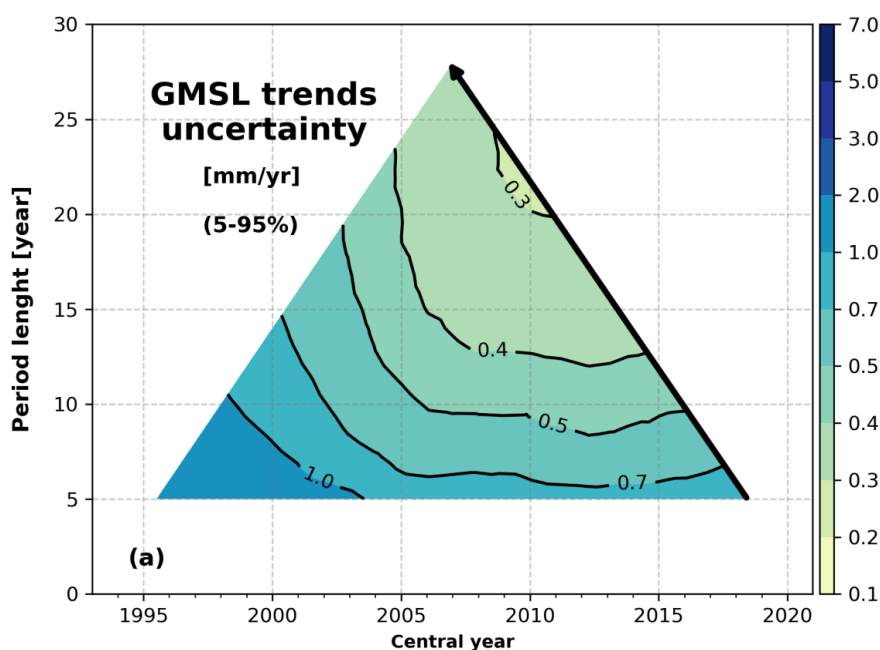


Figure 1: Uncertainty in global mean sea level trends computed over any period > 5 years included in 1993-2020 (adapted from Guérou et al. 2022, the central year of the period used to compute the

trend is in the x-axis and the length of the period is in the y-axis), extracted from Meyssignac et al. (2023).

The GMSL trend uncertainty is around 0.7 mm/yr (90% CL) for 10-yr trends and down to 0.3 mm/yr (90% CL) for 28-yr trends. GMSL uncertainty estimates show a decrease from 9 mm (90% CL) in 1993 to 3 mm (90% CL) in 2015 (see Figure 1). The uncertainty in sea level trends decreases as the period of the trend calculation increases due to the different sources of noise that decorrelate on long time scales. The partitioning of the GMSL trend uncertainty among the different sources of error changes with time scales. For short trends, the uncertainty due to the GMSL offset between TopEx-A and TopEx-B, the uncertainty due to the high frequency correlated noise and the wet troposphere correction (WTC) uncertainty dominate, and for long trends, systematic errors that are correlated at long time scales tend to dominate (see Figure 2). Additionally, the date at which the trends are computed matters.

Regionally, the uncertainty in sea level trends shows a spatial structure, with trends most reliable at high latitudes and far from the coast. In terms of acceleration accuracy, the GMSL record shows pretty much the same spatio-temporal structure as for the trends.

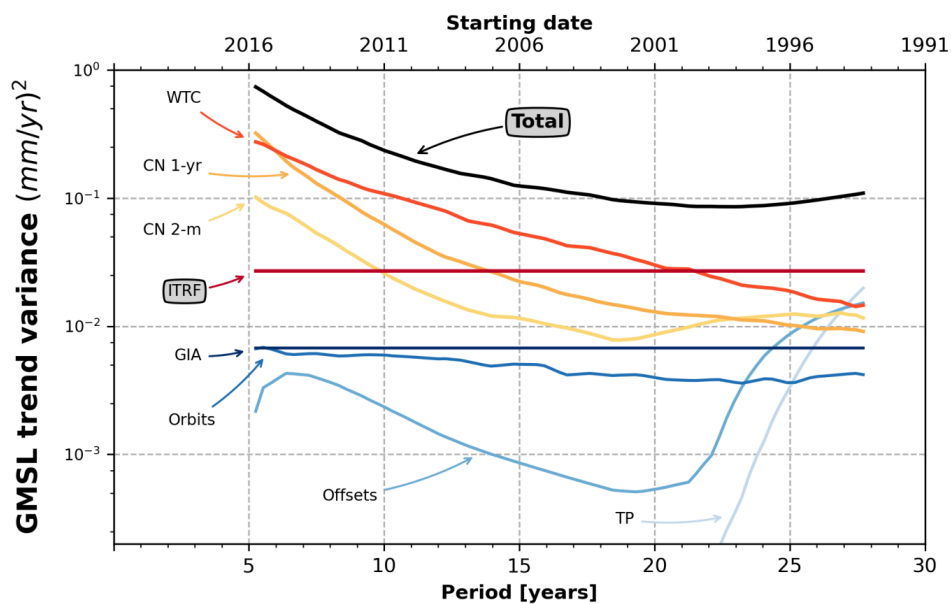


Figure 2: Uncertainty at the 66% CL in sea level trends computed over different length periods that are all ending in 2020 and partitioning of the uncertainty among different sources: 2-months and 1-year correlated noises ("CN 2-m/1-yr", coming essentially from the radar altimeter errors), the radiometer WTC, the intermission offsets, the GIA, the ITRF, extracted from Meyssignac et al. (2023).

### 2.2.3. Future needs in accuracy and precision

The advancements in high-precision satellite altimetry over the years have significantly improved the precision, accuracy, uncertainty, and stability of sea level estimates. The current accuracy and precision are capable of closing the SLB with uncertainties that help identify the causes of sea

level rise. At interannual time scales, the residual of the SLB (sea level minus thermal expansion and ocean mass changes) does not exceed  $\pm 2$  mm (90% CL, see Table 3). For 20-yr and longer trends, the residual remains within  $\pm 0.3$  mm/yr (90% CL). These values fall within the uncertainties of various data sources such as Argo, satellite gravimetry, and satellite altimetry, confirming that the budget is closed. The rise in GMSL over 1993-2018 can be attributed to ocean thermal expansion (46%), glaciers (19%), Greenland ice loss (15%), and Antarctica ice loss (9%) and land water storage variations (11%) (Fox-Kemper et al., 2021).

While the current level of uncertainty in GMSL is small enough to detect and attribute the part of sea level rise due to GHG emissions, it is still too large to identify smaller contributions from land water storage or deep ocean warming (Slangen et al., 2016). These contributions, which provide insights into freshwater trends and the ocean's heat uptake, currently have uncertainties of around  $\pm 0.2$  mm/yr (90% CL) for 20-yr and longer trends (WCRP Global Sea Level Budget Group, 2018). However, these uncertainties are expected to increase in the future. To detect and quantify these smaller contributions, a measurement's accuracy should be no worse than approximately 50% of the expected signal to detect it and 10% to quantify it (Wunsch, 2016). Therefore, an accuracy of  $\pm 0.1$  mm/yr (90% CL) would be sufficient to detect the contributions of deep ocean warming and land water storage, while an accuracy of  $\pm 0.02$  mm/yr (90% CL) would be enough to quantify them (see Table 3).

Climate Science Question	Accuracy in GMSL rates in mm/yr	Accuracy in GMSL acceleration in mm/yr per decade	Accuracy in regional sea level rates in mm/yr on 20-yr trends
Closing the sea level budget	Detection <sup>1a</sup> : $\pm 0.1$ mm/yr - Quantification <sup>1a</sup> : $\pm 0.02$ mm/yr		Detection <sup>2</sup> : $\pm 0.3$ mm/yr Quantification <sup>2</sup> : $\pm 0.07$ mm/yr
Detecting and attributing the signal in sea level that is forced by GHG emissions	Detection <sup>3a</sup> : $\pm 1.5$ mm/yr - Quantification <sup>3a</sup> : $\pm 0.7$ mm/yr		Detection: $\pm 0.5$ mm/yr Quantification: $\pm 0.1$ mm/yr
Estimating the EEI	Detection <sup>4b</sup> : $\pm 0.1$ mm/yr Quantification <sup>4b</sup> : $\pm 0.03$ mm/yr	Detection <sup>5b</sup> : $\pm 0.5$ mm/yr per decade Quantification <sup>5b</sup> : $\pm 0.1$ mm/yr per decade	

Table 3: Science questions and their needs in terms of sea level estimates' accuracy, from Meyssignac et al. (2023).

<sup>1</sup> in order to identify contributions from land water storage and deep ocean warming;

<sup>2</sup> in order to identify the regional distribution of the contribution to sea level from land ice melt;

<sup>3</sup> calculated from (Slangen et al., 2016). These requirements are already met by the current altimetry observing system;

<sup>4</sup> correspond to detection and quantification of decadal changes in mean EEI of the order of  $\pm 0.1 \text{ W.m}^{-2}$ ;

<sup>5</sup> correspond to detection and quantification of trends in mean EEI of the order of  $\pm 0.4 \text{ W.m}^{-2}$  per



decade;

<sup>a</sup> Values apply to 10-yr and longer periods;

<sup>b</sup> Values apply to 20-yr and longer periods.

At the regional scale, the amplitude of the sea level signal is larger than at the global scale, and local sea level departures from the global mean are primarily influenced by thermosteric sea level changes (Forget and Ponte, 2015) and salinity changes in high latitude regions (Hamlington et al., 2020). The impact of mass changes is much smaller and hardly detectable in observations. The local uncertainty in sea level typically ranges from  $\pm 0.5$  mm/yr to  $\pm 6$  mm/yr for 20-yr trends. In certain regions, particularly mid to high latitudes and the Indian Ocean, the local sea level budget does not close by several mm/yr, exceeding the uncertainty of satellite altimetry. To detect and quantify the manometric sea level departures around the global mean and close the sea level budget at the local scale, an uncertainty of  $\pm 0.3$  mm/yr (for detection) and  $\pm 0.07$  mm/yr (for quantification) is required for 20-yr and longer trends (see Table 3). For the detection and quantification of the local forced sea level response to GHG emissions, a similar level of uncertainty is needed. Climate models indicate that the locally forced response in sea level amounts to approximately  $\pm 1$  mm/yr for 20-yr and longer trends (Fasullo and Nerem, 2018), suggesting that a local accuracy of  $\pm 0.5$  mm/yr (for detection) and  $\pm 0.1$  mm/yr (for quantification) on 20-yr trends would be sufficient.

The closure of the SLB has also been utilized to estimate the EEI, which characterizes the radiative imbalance at the top of the atmosphere (Hakuba et al., 2021; Marti et al., 2022; Meyssignac et al., 2019). The EEI represents the heat uptake of the climate system responsible for current climate change (of about  $0.5-1\text{W/m}^2$ ). The precision of measurements from the Clouds and the Earth's Radiant Energy System (CERES) project allows for the evaluation of small changes in the EEI induced by natural or anthropogenic forcing (Loeb et al., 2018b). While the precision of measuring the EEI is evaluated at  $\pm 0.17$   $\text{W/m}^2$  (90% CL) on interannual time scales, the accuracy of CERES is limited by a potential bias of about  $\pm 2$   $\text{W/m}^2$  (Loeb et al., 2018b). The ocean heat uptake (OHU), representing the excess energy stored in the ocean, serves as a precise proxy for the EEI. Satellite altimetry and space gravimetry currently enable the estimation of OHU with an uncertainty of  $\pm 0.2$   $\text{W/m}^2$  at the global scale over 15-yr periods. At decadal time scales EEI experiences changes of the order of  $0.3$   $\text{W.m}^2$  in response to climate internal modes such as the Pacific decadal oscillation (Loeb et al., 2018a) and changes of the order of  $0.1$   $\text{W.m}^2$  in response to hiatus like the one experienced in the early 2000s (Loeb et al., 2018b). Detecting EEI decadal changes of  $0.1$   $\text{W.m}^2$  and trends of  $0.4$   $\text{W.m}^2$  per decade (Loeb et al., 2021) requires an uncertainty in the sea level budget of  $\pm 0.12\text{mm/yr}$  (resp  $\pm 0.03\text{mm/yr}$ ) for decadal trends and  $\pm 0.5$  mm/yr per decade for decadal accelerations. Reaching this level of accuracy would not only enhance our understanding of climate change but also enable monitoring of the physical climate system's response to mitigation policies earlier than other indicators like sea surface temperature.

## 2.3. Overview of available data, including new CCI ECVs

Table 4 summarizes the datasets available for each component. Improvements expected in the SLBC\_cci+ project are outlined in bold. Following the first phase of the SLBC\_cci project, the main

objectives of the SLBC\_cci+ project are to produce an updated global mean sea level budget, over 1993-2023 and to produce a sea level budget at regional scale, requiring gridded variables.

It is expected to focus on the available CCI essential climate variables (ECVs). These include ice sheet mass loss timeseries, atmosphere water vapor content variations and some components of the terrestrial water storage variations (soil moisture, snow, lakes). Even though these CCI ECVs rarely cover the full altimetry era, they may help compute the components over the time span they are available. Land water storage variations cannot be fully reconstructed from CCI ECVs due to the lack of some contributions such as the groundwater storage variations. However, the relative contributions of soil moisture, snow cover and lakes to LWS variations, to ocean mass change and to GMSL variations, can be assessed using the corresponding available climate data records (CDRs) of ECV.

Tasks	Component	Data
2100	Total sea level from altimetry	C3S (from SL_cci) 1993-present <b>SLBC_cci+: improved Jason-3 wet troposphere correction</b>
2200	Steric sea level from in-situ observations	(Dieng et al., 2017) 1993-2016 SLBC_cci 2002-2016 ISAS17/ISAS20 Ifremer 2002-2020 <b>SLBC_cci+: climatology, time series update until 2023</b>
2300	Ocean mass from satellite gravimetry	Mascon solutions from GSFC, JPL, CSR 2002-2022 Estimates based on spheric harmonic solutions (CSR, ITG, COST-g) 2002-2022
2410	Glaciers	Bamber et al., 2018 (Hugonnet et al., 2021) since year 2000 <b>SLBC_cci+: time series update until 2023 (Dussaillant et al., 2023)</b>
	Ice sheets	<a href="#">CCI 2002-2017 (Greenland)</a> , <a href="#">2002-mid-2020 (Antarctica)</a> IMBIE 1993-2020, new release expected
2420	Land water storage	SLBC_cci / WaterGAP 1993-2016 expected to be extended till 2019 ISBA-CTRIP 1993-2018 (Humphrey and Gudmundsson, 2019) 2002-mid-2019 Other global hydrological models will be also considered (eg, LAD model from GFDL)
	Atmospheric Water Vapour	HOAPS 1993-2020 over ocean, <a href="#">CCI 2002-2017 over land</a> ECMWF model reanalyses (e.g; ERA-Interim, ERA5) 1993-2022
2500	GIA and fingerprints	Series of GIA models computed using Spada and Melini (2019) and present day ice melting fingerprints <b>SLBC_cci+: improved spatial resolution</b>
2600	Synthetic observations	Models and reanalyses output from OSTST-IMHOTEP project 1993-2018 <b>SLBC_cci+: extraction of synthetic data at the times and locations of the various observation measurements above</b>

Table 4: Available datasets for the sea level budget components. Improvements foreseen in the SLBC\_cci+ projects are indicated in bold font. Available CCI ECVs are written in blue.

The IMOTHEP ocean model provides synthetic data consistent for in-situ (including Argo), satellite altimetry and satellite gravimetry observations. Therefore, synthetic data from the IMOTHEP ocean model have the potential to bring insight to the error linked to the observability of the systems involved in the budget.

## 3. Specific requirements for the Arctic Ocean

### 3.1. State-of-the-art of the Arctic sea level budget closure

The results of the first phase of the ESA SLBC Project revealed fundamental insights into the global mean sea-level budget and the Arctic Sea Level Budget. Based on the current observing systems used for partitioning the components of the sea-level budget and model-based information for assessing the contribution of glaciers and water storage anomalies, (Horwath et al., 2022) underlined that global mean sea-level trend agrees with the sum of the steric and mass components within their combined uncertainties (10 % of sea-level rise). The results on the Arctic sea-level budget assessment, obtained during the same phase of the Climate Change Initiative, show instead a different scenario where large departures from the global assessment can be observed. Raj et al. (2020), focusing on the sea-level budget assessment in the Arctic during the Grace/Argo era, observed a residual trend larger than  $1 \text{ mm yr}^{-1}$  based on the sum of the sea-level budget components compared to the sea-level rates obtained from altimetry. Figure 3 shows the comparison of the variability in the altimeter derived sea level of the entire Arctic Ocean to the sum of observed changes in steric sea level height and ocean mass change. The residual between the two estimates clearly show the sea-level budget disclosure in the Arctic region. Furthermore, the authors underlined that the observed sea-level budget disclosure can be attributed to the observing capabilities in the Arctic region, which are limited compared to other areas of the global ocean. Specific recommendations of Raj et al. (2020) included: (i) Improved summer retrievals in sea ice covered areas from satellite altimetry by gaining better understanding of the radar altimeter response over the different ice types; (ii) update the ocean mass change data using state-of-the-art solutions, for example by using the new Global tailored-kernel solutions with higher resolution and including leakage-regions near the coast as well; (iii) improved estimation of the steric component through incorporation of more/all-available in-situ observations with better coverage.

The following Sections detail about the requirements based on the above mentioned recommendations.

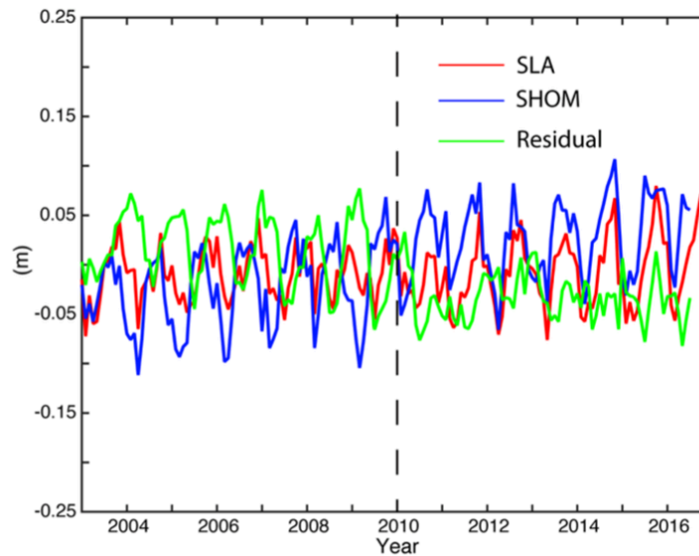


Figure 3: Arctic Sea level Budget: Area averaged monthly sea level (red), the sum of GSFC ocean mass change and the EN4 steric height estimates (SHOM, blue), and the residual (green) for the entire Arctic during the time period 2003–2016. The dashed vertical line indicates the separation of the time periods 2003-2009 and 2010-2016 when changes in the dominant atmospheric patterns over the Arctic are observed (from Raj et al., 2020).

### 3.2. Requirements for the altimetry components and ways for improvement

Monitoring the Arctic Ocean is non-trivial. The Arctic observing network is notably lacking the capability to provide a full picture of the changing ocean due to e.g. limitations to sample the sea-surface in the marginal ice zones and sea-ice covered areas. Figure 4 shows the spatial variability of the sea-level anomaly trend (a) in the Nordic Seas and in the Arctic Ocean during the period 2003-2016, as well as sea level anomaly (SLA) trends of percentiles 2.5% (b) and 97.5% (c) for the same time period. The maps clearly show the positive sea-level rates in the Nordic Sea and Beaufort gyre. The authors found that sea-level rise in the Nordic Sea areas was mainly driven by thermosteric sea-level, while the halosteric sea-level variation due to ocean freshening led to the positive trends in the Beaufort Gyre. The trend maps also shows how conventional altimetry is affected by reduced observing capabilities in the Arctic Ocean resulting in a lack of measurements in the Polar region (Polar Gap). This leads to the obvious need of optimizing the exploitation of data from space-borne sensors. Two-main initiatives, ESA funded (Cryo-TEMPO project) and the CNES funded (AltiDoppler project) are progressing in this direction.

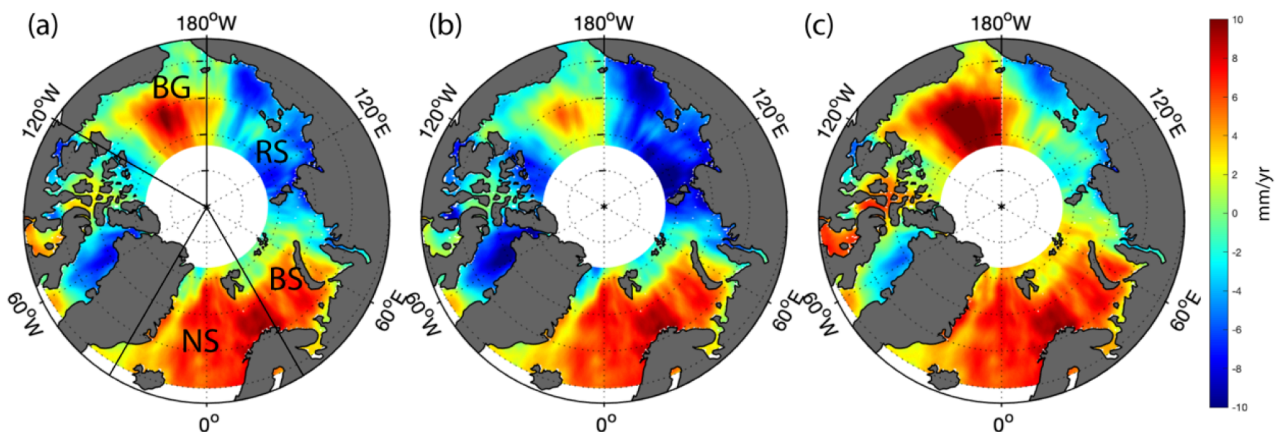


Figure 4: The panels show the Sea level anomaly (SLA) trend (mm/yr) for the time period 2003–2016 with the marked locations of the Beaufort Gyre (BG), the Nordic Seas (NS), Barents Sea (BS) and the Russian shelf region (RS). SLA trends (mm/yr) of percentile 2.5% (b) and 97.5% (c) for the same time period. The sea level anomaly trend for the time period 2003–2016 with the marked locations of the Beaufort Gyre (BG), the Nordic Seas (NS), Barents Sea (BS) and the Russian shelf region (RS); The trend estimates are obtained from conventional altimetry maps; values expressed as mm yr<sup>-1</sup> (from Raj et al., 2020).

### 3.2.1. The ESA Cryo-TEMPO Project

The Cryo-TEMPO project brings together a team of radar altimetry scientific experts and software engineers, to generate agile and state-of-the-art thematic data products. The figure shown below is produced from a CryoTEMPO data set containing CryoSat data from the SAR and SARIn modes, and it is processed with a Threshold First Maximum Retracker Algorithm (TFMRA), adjusted to the polar ocean studies. The newly reprocessed Cryosat altimeter data reproduces all main circulation features of the Arctic. The Beaufort Sea and the Eurasian Basin are characterized respectively by high and low sea level, the difference between them reaching up to 1.0 m. The spatial pattern and ADT gradients also indicate precise positioning of the well-known transpolar drift stream in the Arctic. A main noticeable improvement in the new Cryo-Tempo data in comparison to other altimeter data (e.g., CMEMS data; Figure 5) is the significant improvement in the availability of quality altimeter data in the central Arctic, thereby reducing the “polar gap”, a well-known issue associated with the estimation of altimeter derived sea level in the Arctic.

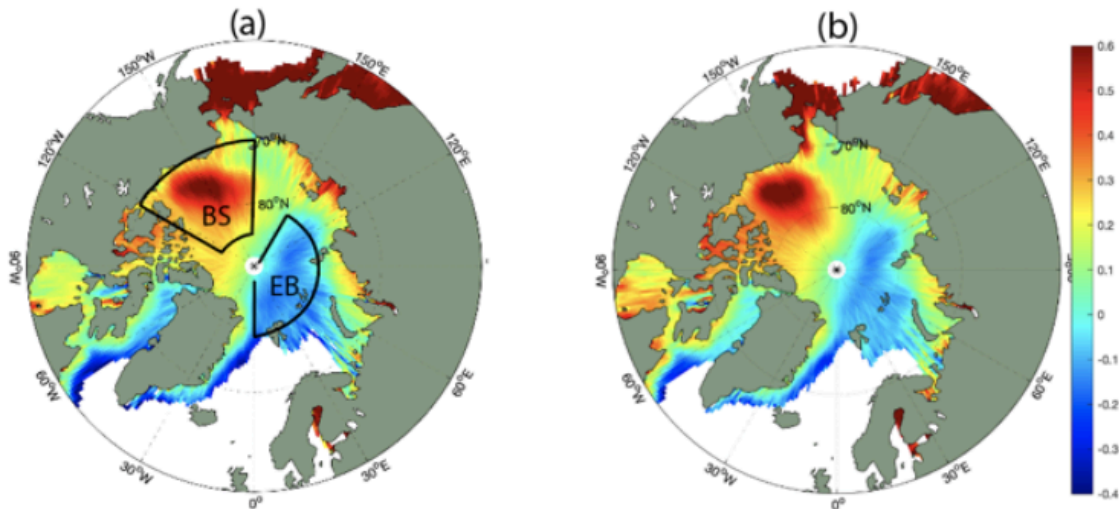


Figure 5: Sea-level anomaly (cm) in the Arctic. The values show the sea-level anomalies, averaged over a period spanned by the Cryosat and Cryosat-2 missions (2010-2021). The map is obtained by binning (every 1-degree longitude and 0.5-degree latitude bins) along-track data of the altimetry missions which have been reprocessed, in the framework of the ESA Cryo-Tempo project to account for the sea-level signal in the sea-ice covered areas and reduce the polar gap. The black frames represent the Beaufort Sea (BS) and the Eurasian Basin (EB) domains.

### 3.2.2. Enhanced altimetry to obtain sea-level signal in sea-ice covered areas

Newly reprocessed along-track measurements of Sentinel-3A, CryoSat-2, and SARAL/AltiKa altimetry missions (AVISO/TAPAS), optimized for the Arctic Ocean (Prandi et al., 2021), have also been recently produced in the framework of CNES AltiDoppler project (Figure 6).

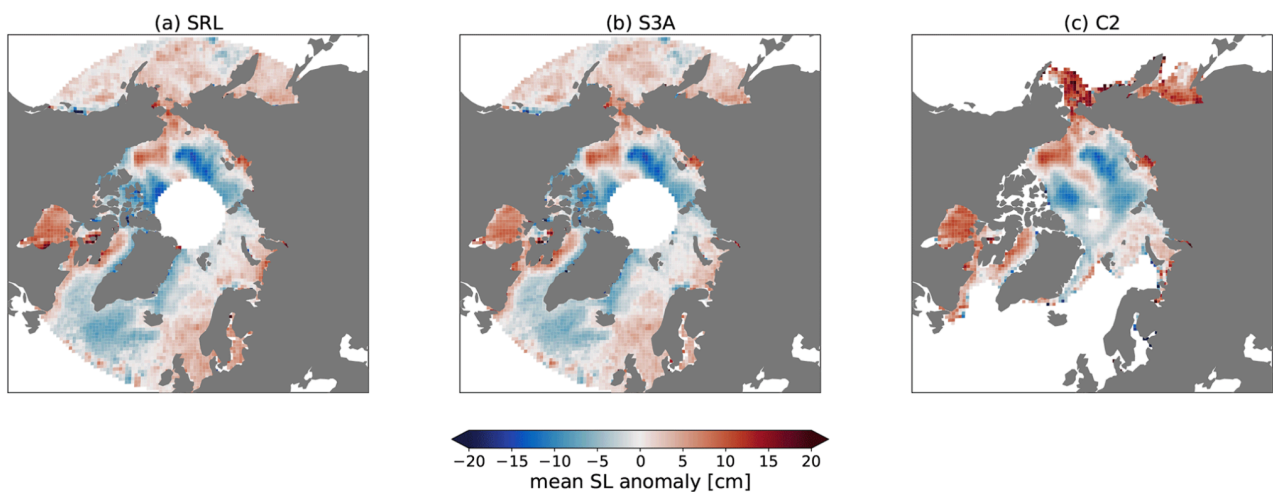


Figure 6: Mean Arctic SLA maps for SRL (a), S3A (b) and C2 (c). All maps are estimated over the time span common to all missions (July 2016–April 2019) (Prandi et al., 2021).

The time-series of the reprocessed along-track data were recently updated to cover the lifetime of the three missions (2011-2021; [10.24400/527896/a01-2020.001](https://doi.org/10.24400/527896/a01-2020.001)). The latter allows for novel estimates of sea-level trends in the Arctic based on enhanced altimetry signals over the last decade with reduced uncertainties.

### 3.2.3. The Sea Water and Ocean Topography (SWOT) Mission

The SWOT Mission was launched in December 2022. The SWOT mission extends the capability of existing nadir altimeters to two-dimensional mapping and sampling of the ocean surface at an unprecedented spatial resolution (e.g. (Bonaduce et al., 2018)). The fast sampling phase of the mission offers the unique opportunity to observe the high temporal resolution of the ocean features resolved by SWOT at unprecedented spatial resolution. Even though the orbit of the mission is not optimal for measuring sea-level at the high latitudes, it covers critical areas in the Nordic Seas where the modulation of heat transported by the Atlantic Waters on their pathways to the Arctic. For example, the 1-day repeat orbit shows a cross-over located in the Lofoten Vortex (see Figure 8) which is an area considered as an hot spot of mesoscale activity in the Nordic Seas (Raj et al., 2016; see Figure 6). During its science phase the SWOT mission will cover those areas of the Nordic Seas every ~20 day bringing new insights into the sea-level variability: e.g. it will allow to assess how resolving the sea-level anomaly field at fine scale will improve the capabilities of resolving the monthly sea-level variability, compared to our current knowledge base on conventional altimetry.

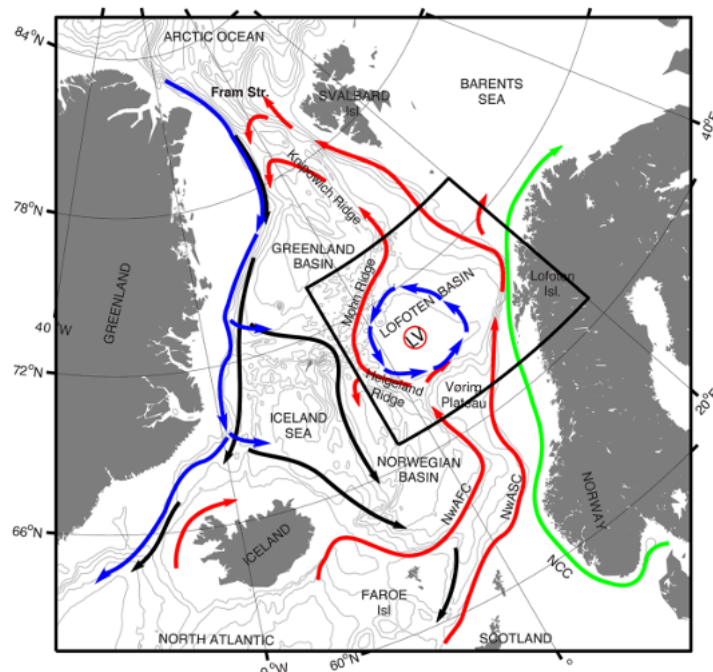


Figure 7: The black outlined area including the Lofoten Basin shows the geographical domain where satellite sensor synergy data are collocated with Argo profiling floats. Arrows mark the flow directions of the Norwegian Coastal Current (green), Norwegian-Atlantic Current (red) East Greenland Current (blue) and Deep overflow water (black).

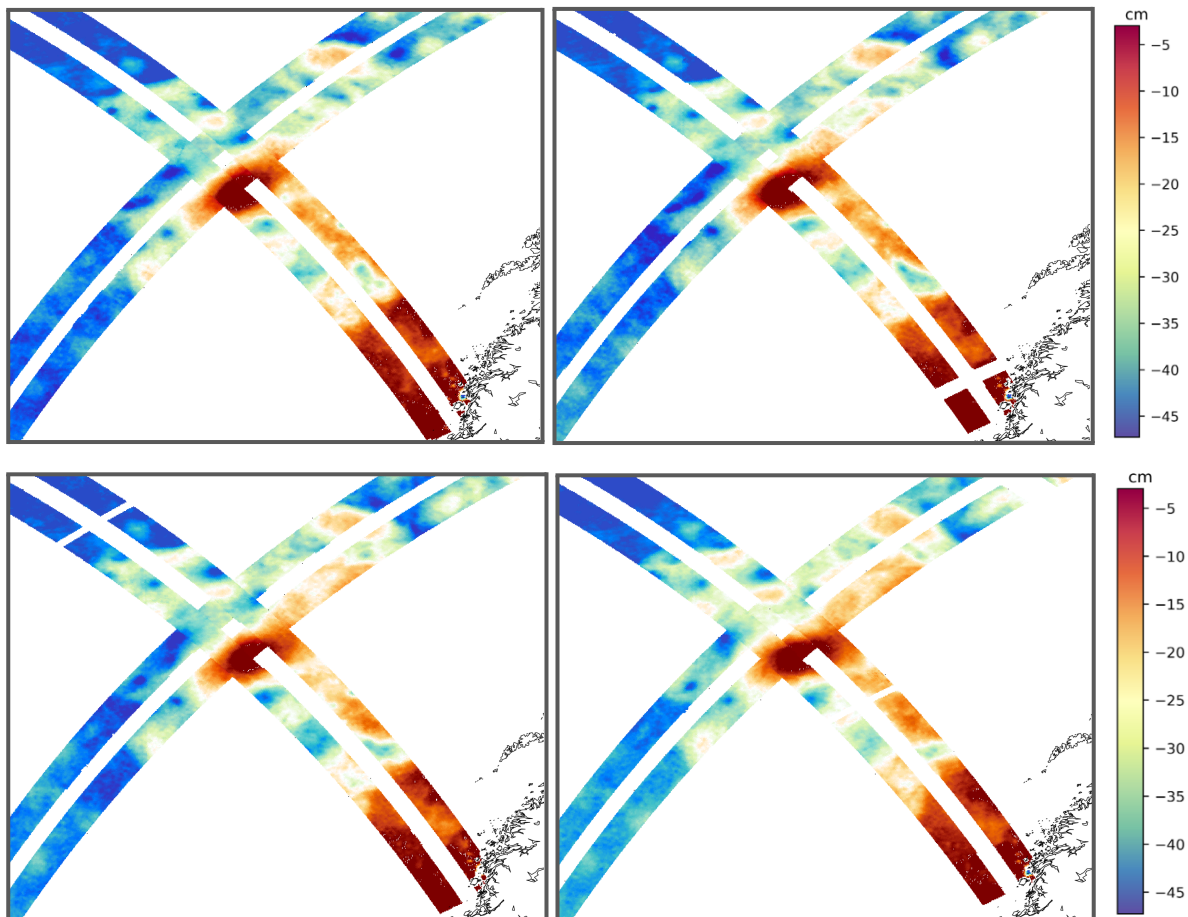


Figure 8: The panels show the SWOT KaRIN image in the Lofoten Basin during four consecutive days in May 2023 (8th-11th May 2023, clockwise from top-left). The patterns show the variability of the absolute dynamic topography (ADT) in the area. While the processing of SWOT KaRIN images is still preliminary, early images can be accessed through a dedicated bulletin for a number of early adopter initiatives:

([https://bulletin.aviso.altimetry.fr/html/produits/swot/adac/welcome\\_uk.php](https://bulletin.aviso.altimetry.fr/html/produits/swot/adac/welcome_uk.php)).

### 3.3. Requirements for the gravimetry components and way forward

In the ESA SLBC project (Phase 1), two main types of remote sensing-based solutions of ocean mass change derived from the GRACE gravimetry data by means of mascons and spherical harmonics (SH) are estimated. Both solutions represent mass changes over the ocean, which is expressed as monthly surface-density change, corresponding to millimeters of equivalent water height at 1000 kg/m<sup>3</sup> density. The application of SH-type solutions offers the benefit of an unconstrained data approach, whereas mascons already include localized pre-assumptions and a priori constraints on spatial-temporal mass variance. However SH-type solutions have two main disadvantages: (1) smoothing (Gaussian filtering and destriping) leads to substantial signal dampening and reduced linear trends (Johnson and Chambers, 2013), and (2) signal leakage and indistinct separation of the land-ocean boundary enforces the application of a ~300 km wide buffer



zone. The latter is of fundamental relevance in the Arctic, where the bulk of recent ice mass loss occurs and is reflected in strong coastal leakage. An illustration of this is shown in Figure 9. The SH-type solutions shown in the Figure is based on ITSG-Grace2018 unconstrained Level-2 monthly solutions up to degree and order 60 by the Institute of Geodesy at Graz University of Technology (ITSG; (Kvas et al., 2019)) and were subsequently post processed during the ESA CCI SLBC project for ocean mass change. Mascons (GSFC solution shown in the figure; (Luthcke et al., 2013)), on the other hand provide a way to enforce a sharper separation of mass changes on either side of the boundary and do not involve coastal buffer zones against leakage. Mascon solutions (Loomis et al., 2019) have also been recently used to assess the mass component of sea-level variations along the Norwegian coast (Mangini et al., 2023). The results show that gravimetry data are reliable in shelf areas, when compared with indirect manometric sea-level estimates obtained from the combination of satellite altimetry and in-situ data from hydrographic stations.

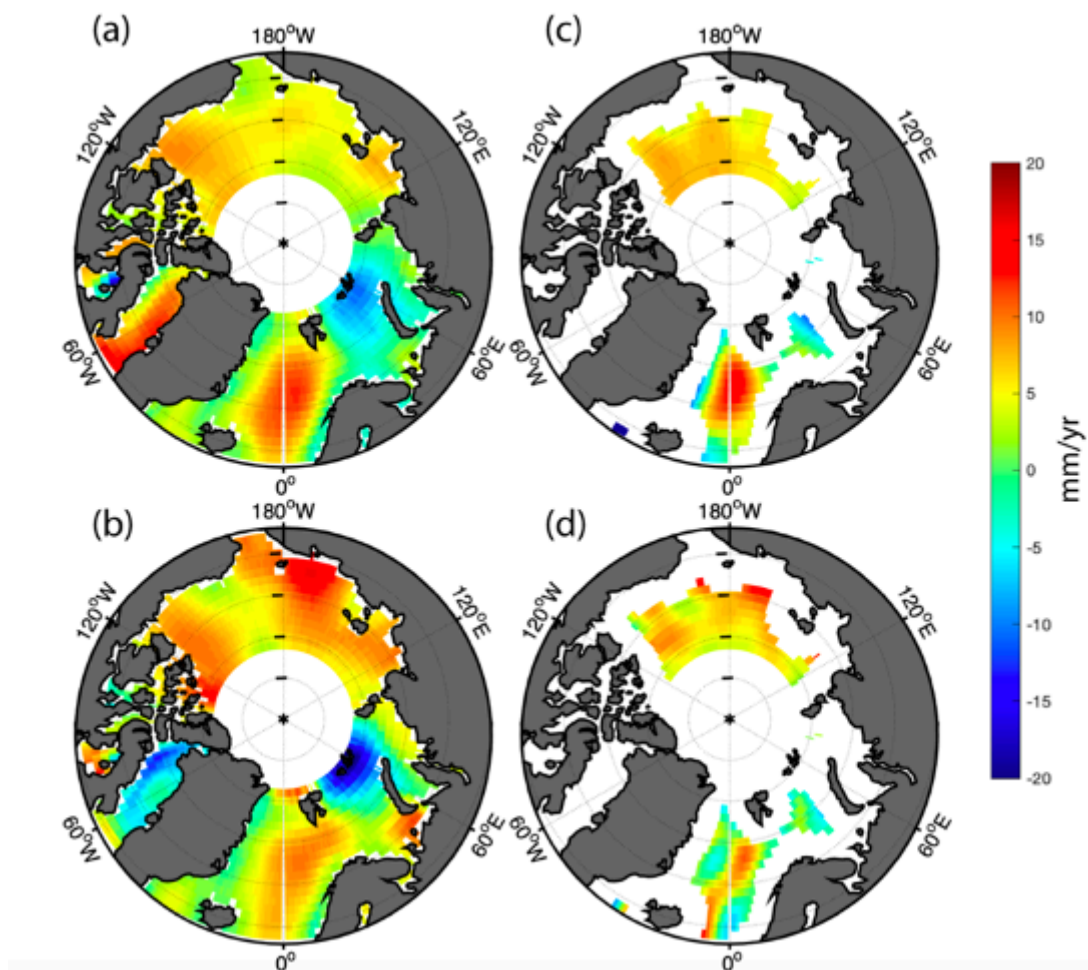


Figure 9: GSFC (left panels) and ITSG (right panels) derived ocean mass trend during the two time-periods 2003-2009 (upper panels) and 2010-2016 (lower panels).

One of the recommendations to take benefit of the unconstrained SH-solutions for the ocean mass changes may be the development of a new tailored-kernel solution for ocean mass change from

GRACE data, based on an approach by Groh and Horwath (2016) that has been utilized for the Antarctica region.

## 3.4. Requirements for in-situ observations and way forward

### 3.4.1. Tide gauges

Tide gauges have been fundamental in highlighting the trend in the rise in sea levels in the last century (Douglas, 1991, 1997). Tide-gauge records have also always been used to calibrate altimeter sea level measurements, in order to obtain a highly accurate mean sea level (Leuliette et al., 2004; Mitchum, 1994, 1998, 2000) over last decades. On the other hand, their spatial distribution is sparse and data records can be affected by errors (e.g. instrumental) and large gaps due to the size of the tide-gauge observing network that has experienced large fluctuations over long temporal windows covered by the in-situ measurements. This scenario applied well to the Arctic where the availability of tide-gauge stations is affected by the difficulties in deploying and maintaining tide-gauge instruments in remote geographical locations, as well as by the data access policies applied by the countries which are facing the Arctic Ocean. This leads to a distribution of in-situ measurements which can be discontinuous both in time and in their geographical distribution. Figure 10 shows the distribution of tide-gauge stations and data available, provided by the Permanent Service for Mean Sea Level (Holgate et al., 2013) in the Nordic Seas and in the Arctic Ocean considering a time window which overlaps the satellite altimetry era (1993-2022).

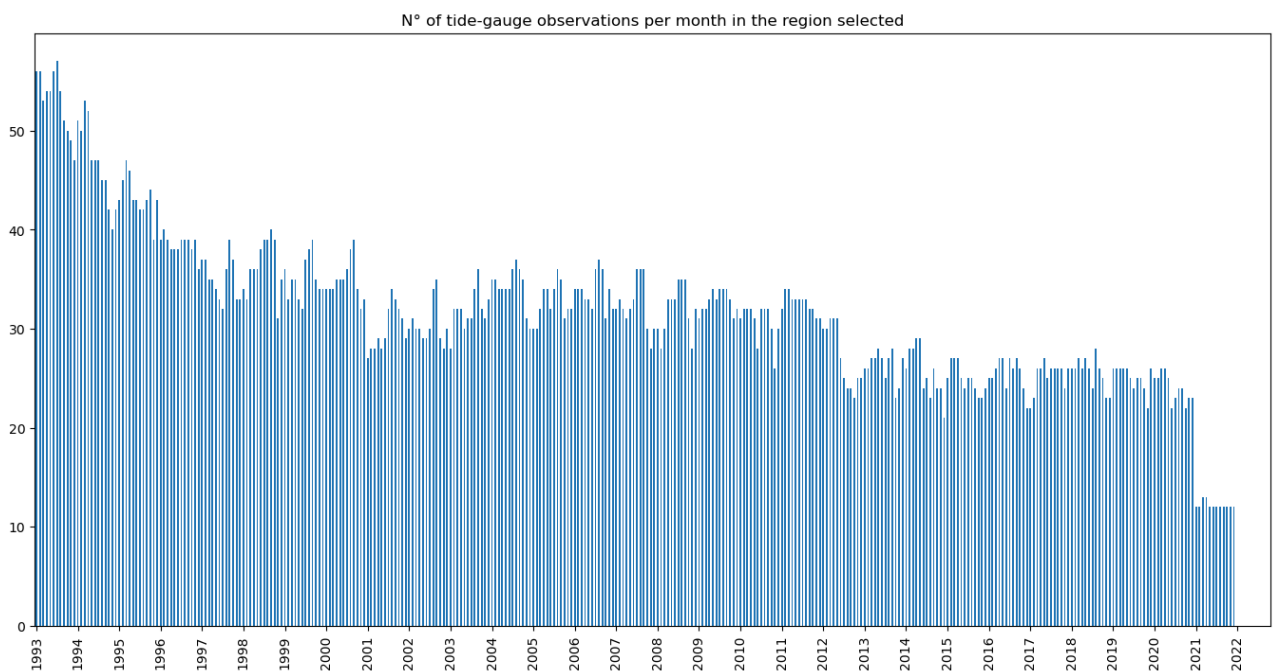
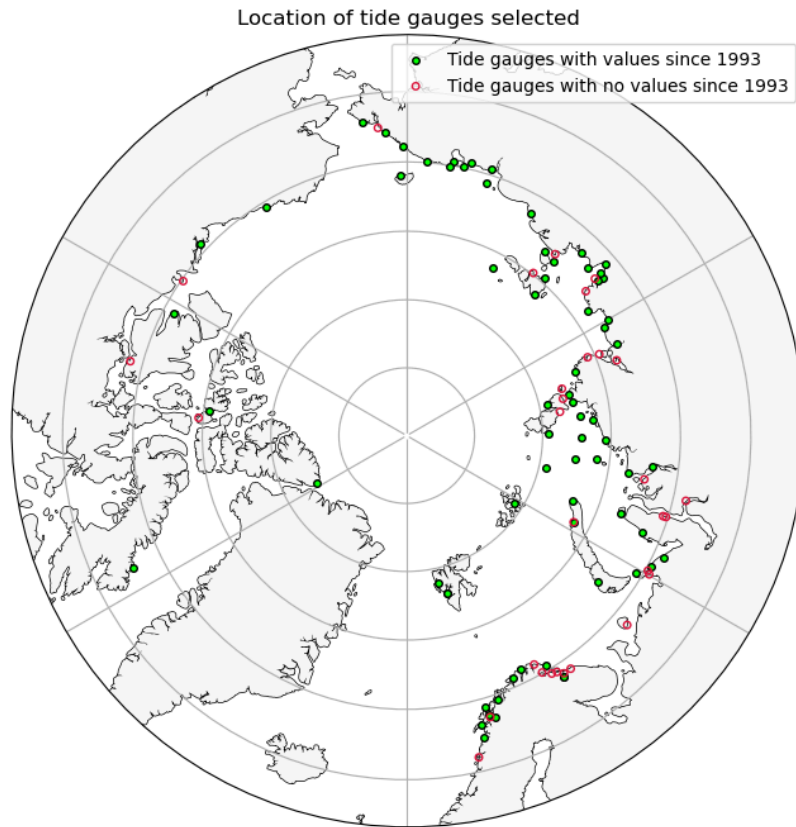


Figure 10: Top panel: Map showing the location of the PSMSL tide gauges in the Arctic region (defined as the region to the north of 66°N). Bottom panel: A bar chart with the number of tide-gauge observations in the Arctic region for each month between January 1993 and December 2022 (PSMSL tide gauges do not contain values after Dec 2021). Two out of the one hundred PSMSL tide gauges do not contain values over the period considered. These two tide gauges are located near the border between Norway and Russia. Their location is shown on the map with empty red circles.

A way forward will be to focus on recent efforts aimed to compile an Arctic Atlas for Tidal constituents (Hart-Davis et al., 2023) based on tide gauges, ocean bottom pressure sensors and GNSS-R. The data-set includes 2000 sites of measurements, ~900 sites above 60°N and ~400 above 70°N with a much greater spatial distribution across the full Arctic Ocean. Accessing the time-series used to estimate tidal-constituents will bring to a novel assessment based on in-situ measurements in areas of the Arctic which are still poorly sampled.

### 3.4.2. New phases of the NorArgo Programme

NorArgo is funded by the Norwegian Research Council for 2018-2023 (through the infrastructure project NorArgo2). The main objective of NorArgo2 is an ocean observing system for the Arctic that will monitor essential physical and ecosystem variables at ~weekly temporal resolution. NorArgo3 will extend the existing NorArgo2 infrastructure, which will include a new generation of Argo floats and novel biogeochemical sensors. NorArgo3 thus will be a sustainable observation system for the Arctic that provides continuous measurements over large areas that are fundamental in climate research and monitoring. The Norwegian Argo floats are part of the international Argo program and the roadmap of Euro-Argo ERIC, that Norway has been a member of since 2018 (Figure 11). The Argo floats are mainly located in the deep water drifting with the currents there. With 5-10 day intervals, they rise from the depth, 2000-4000 m depth, to the surface while taking measurements during the ascent (Figure 12). The floats are equipped with sensors for measuring pressure, temperature, salinity, oxygen concentration and other biogeochemical parameters that are important for the description of the ecosystem. Each Argo float can do approximately 150-200 cycles over 3-5 years. NorArgo3 will operate minimum 30 operative Argo floats, simultaneously drifting in the Nordic Seas, the Barents Sea and the Arctic Ocean. The aim is to monitor changes in the ocean's climate and the properties of the water masses and biological diversity throughout the water column and the deep currents in the ocean. Complementing the Argo Programme, the profiling floats deployed by the NorArgo programme represent the backbone for obtaining reliable estimates of the steric sea-level in the Nordic Seas.

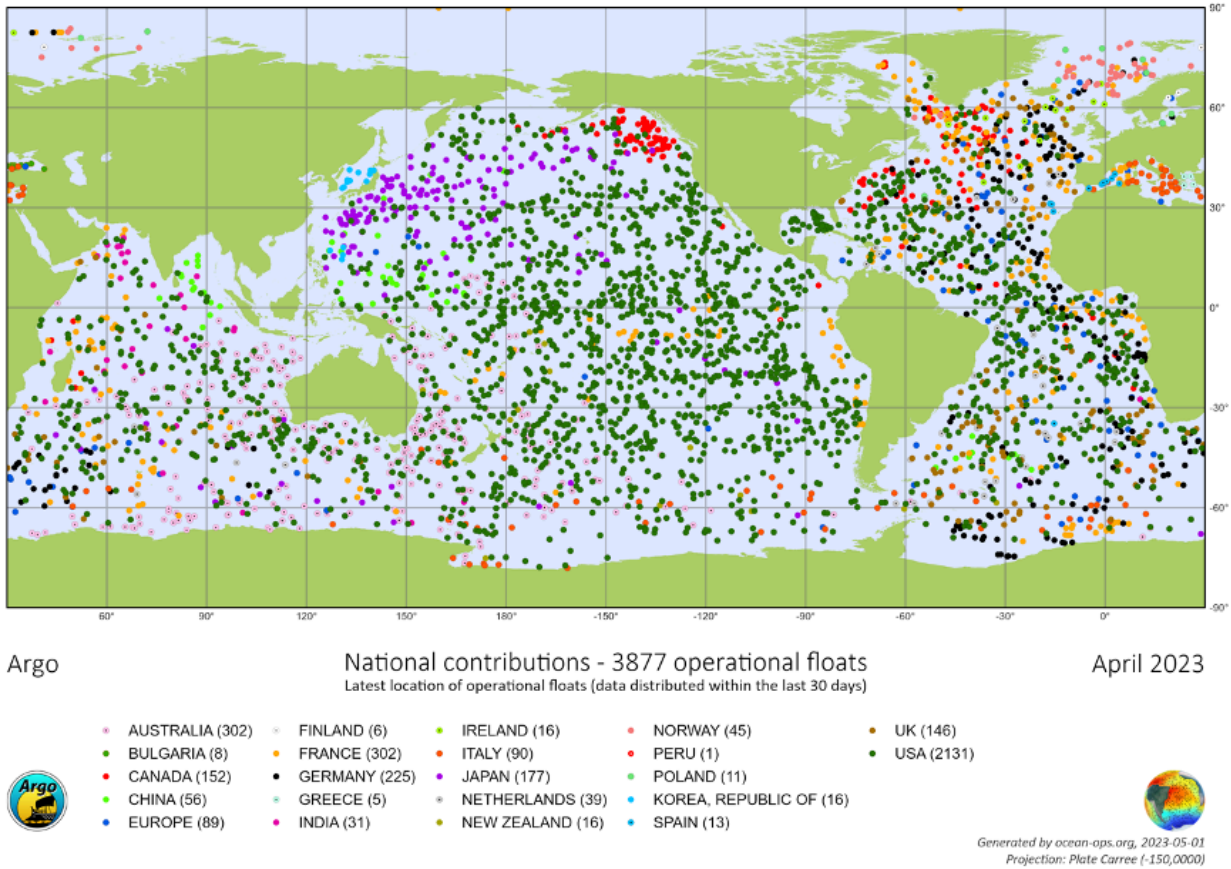


Figure 11: Registered positions of all operative Argo floats in the world ocean (April 2023).

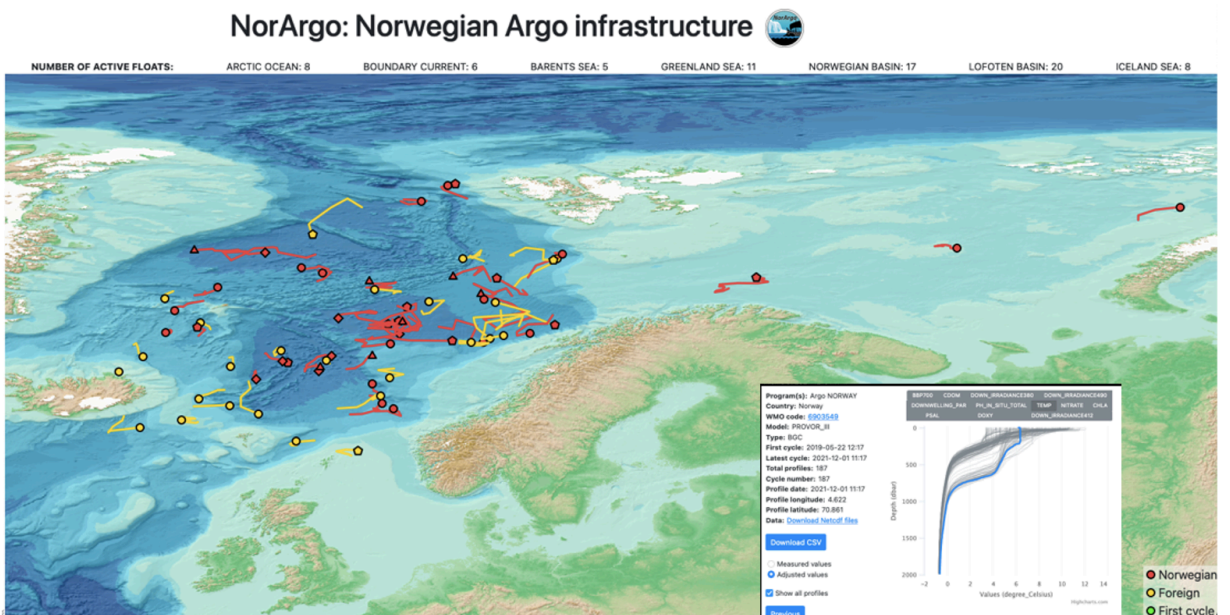


Figure 12: The panel shows an example profiling floats of the NorArgo operating in the Nordic Seas during a day ([www.imr.no/forskning/prosjekter/norargo/map](http://www.imr.no/forskning/prosjekter/norargo/map)).

### 3.4.3. Dedicated initiatives to capitalize on the field campaigns collecting data in the Arctic

#### 3.4.3.1. Beaufort Gyre Exploration Project

The Beaufort Gyre Exploration Project (<https://www2.who.edu/site/beaufortgyre/>) has provided continuous monitoring of conditions in the Beaufort Gyre region since 2003 (Cornish et al., 2023), and established a strong foundation that is vital for understanding the current state and future trajectories of the Arctic Ocean environment. The major goal of this program is to investigate basin-scale mechanisms regulating freshwater and heat content in the Arctic Ocean and particularly in the BG.

#### 3.4.3.2. GoNorth expeditions

The GoNorth expeditions (<https://www.sintef.no/projectweb/gonorth>) took place during different periods of the last years, starting from 2010, pushing the boundaries of knowledge about oceanic areas, from the seafloor and subsea geology to the sea ice, via the water column. The main goal is the exploration of the Gakkel Ridge, the mid-ocean ridge located between Svalbard and the North Pole. The Gakkel Ridge appears on maps as a sort of underwater mountain range that extends about 1800 kilometers, in a roughly straight line, from the northern end of the Fram Strait towards Siberia.

#### 3.4.3.3. HiAOOS Project

The recently funded High Arctic Ocean Observation System (HiAOOS) Project of the Horizon Europe Programme (<https://cordis.europa.eu/project/rcn/243926/en>) aims to advance the uptake of new ocean observing capabilities and capacity in the high Arctic to strengthen European and national infrastructures in their effort to support new and ambitious research within climate, environment and geohazards. HiAOOS will develop, implement, and validate several ocean observing technologies to improve data collection in the ice-covered Arctic Ocean. A network of multipurpose moorings will be deployed for two years in the deep Nansen and Amundsen Basins. The network will provide point measurements of ocean and sea ice and active and passive acoustic data for several applications, including acoustic thermometry.

While sub-optimal for sea-level budget assessment, due to the time-window covered by the different campaigns and expeditions, those are invaluable efforts and represent a unique source for assessing the uncertainties of the components of the sea-level budget during specific periods.

## 4. Summary

Closing the sea level budget enables ensuring that all contributions to sea level rise have been identified, checking that the observing system is robust enough to measure the individual components, verifying that the ECVs are consistent with each other and enables detection and attribution related to GHG. Requirements for the sea level budget presented in section 2.2.3. and Table 3 give the objective we should aim at when assessing the sea level budget residuals. In global mean, the trend of the sea level budget residuals should be estimated with an accuracy of 0.1 mm/yr for detection and of 0.02 mm/yr for quantification. At regional scales, over periods of 20 years, an accuracy of 0.3 mm/yr would be necessary for detection and of 0.07 mm/yr for quantification. Hence, the sum of the variances of all components should remain below the square of the estimated requirements. For each individual component, the requirements are therefore even more stringent.

Within the SLBC\_cci+ project, state-of-the-art data will be used for all components, to ensure the highest possible level of accuracy and precision and to get as close as possible to the scientific requirements. A particular attention will be paid to uncertainty estimates. One of the objectives of the project is to estimate the spatial variations of the sea level budget, from local to regional scales. The sea level budget in the Arctic ocean will be specifically addressed with suitable datasets.